THE JOURNAL OF PHYSICAL CHEMISTRY C

Article

pubs.acs.org/JPCC

Electronic and Magnetic Changes in a Finite-Sized Single-Walled Zigzag Carbon Nanotube Embedded in Water

Carlos M. Ruiz and Sergio D. Dalosto*

INTEC−CONICET and Universidad Nacional del Litoral, Güemes 3450, S3000 Santa Fe, Argentina

Supporting Information

ABSTRACT: In vacuum an open-ended finite-sized zigzag and hydrogen atom terminated carbon nanotube (FS-CNT) has a ground state with antiferromagnetic configuration, and the α and β gaps are degenerated with a magnitude inversely proportional to the nanotube length. However, when a FS-CNT is embedded in a box of water molecules, a single-file hydrogen bonded chain of water molecules (confined water inside) flows through it from one side to the other, while a spatially varying density profile occurs for the bulk water molecules (unconfined water outside). As a consequence, we have observed for an embedded FS-CNT(11,0,L) with L < 2.0 nm important changes in its electronic and magnetic properties. The electronic gap degeneracy is broken, and the gap value for each spin state fluctuates around a mean value which depends on the CNT length. We rationalized these changes by decomposing the fluctuating electric field produced by the water molecules as due to molecules of unconfined water outside and confined water inside the FS-CNT. The confined water inside produces an electric field nearly constant in magnitude and pointing almost along the axial axis of the tube, equivalent to an external uniform electric field with a mean value of 0.56 ± 0.05 V/nm. Meanwhile, the unconfined water outside produces an electric field that fluctuates randomly in direction and magnitude, and it is equivalent to an external uniform electric field with a mean value of 0.7 ± 0.4 V/nm. The maximum electric field observed was 1.7 ± 0.2 V/nm which occurs when both confined water inside and unconfined water outside the electric fields have the same direction. The maximum electric field is three times smaller than the one necessary to change the CNT from semiconductor to half-metallic. The findings are important in devices where solvent molecules change the electronic properties of the CNT.

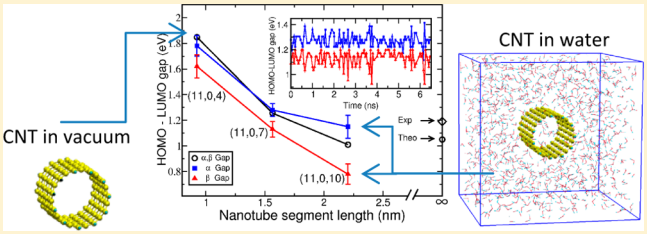

INTRODUCTION

Carbon nanotubes (CNTs) have been used in a wide range of applications including catalysis,[1] electronics, and molecular sensing.[2] In particular, there is a great interest in understanding the structure and transport properties of confined water, ions, and drugs inside of nanometer channels built with CNTs.[3] This is due primarily to the similarity of these properties with those observed in biological systems and also to the important consequences for sensors based on CNTs. In particular, when an open-ended CNT is solvated in a water reservoir, it is spontaneous and continuously filled with water, and the transport of these confined water molecules inside of the CNT occurs. The transport of the confined water inside the CNT can be driven by an external electrostatic field, pressure, and structural deformations among others.[4,5] The structure of the flowing confined water molecules changes drastically as soon as the diameter of the CNT decreases.[6] Specifically, for CNTs with diameters greater than ∼2 nm, the structure of confined water molecules inside resembles, at the center of the CNT, the unconfined behavior, while for diameters of the order of ∼1 nm, the confined water molecules can flow, forming a single-file chain with an ordering path and a well-defined hydrogen bond interaction among them.[7−10] At the same time, the density profile of unconfined water molecules outside the wall of the nanotube is almost invariant with the CNT diameter. Another important aspect of the CNT is its electronic and magnetic properties. In particular, single-walled carbon nanotubes (SWCNTs) can be produced as metallic, quasimetallic, or semiconducting. For finite-sized single-walled CNTs, new interesting features were theoretically predicted. For instance, the HOMO−LUMO gap is degenerated. It decreases oscillating for CNTs with armchair edges, while it shows a monotonic decrease with the length for zigzag edges. For finite-sized and hydrogen atom terminated zigzag CNTs such as (7,0), (8,0), (9,0), and (10,0), their ground state is antiferromagnetic, similar to what occurs for graphene nanoribbons and graphene nanodots; that is, opposite spins are observed at the edges.[11−15] Besides, the HOMO−LUMO gap degeneracy can be broken and also turn the tube to half-metallic by applying an external electric field along the direction of the tube axis.[12] Applying an external electric field in the direction perpendicular to the axial axis of the tube does not break the gap degeneracy, but it is capable of turning the tube to metallic. The consequence of changing the semiconductor state to half-metallic opens the possibility to have a spin-polarized current of fundamental interest in spintronic

Received: August 16, 2012
Revised: December 10, 2012
Published: December 12, 2012

   dx.doi.org/10.1021/jp308174k | J. Phys. Chem. C 2013, 117, 633−638

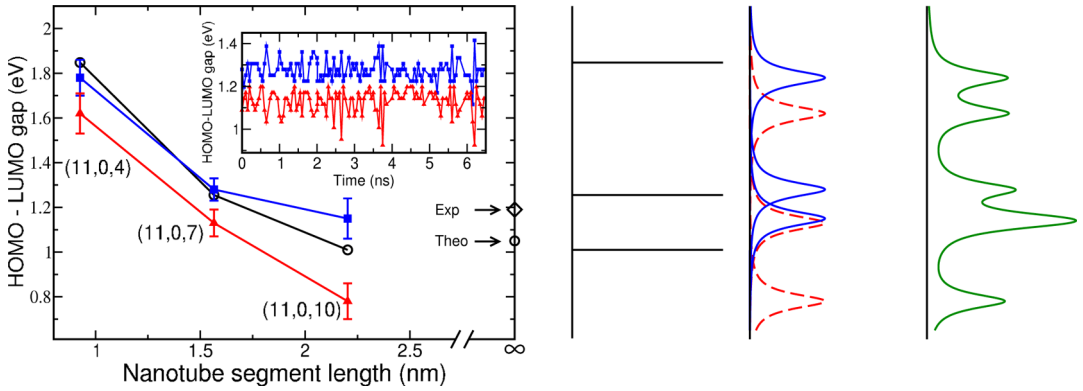

Figure 1. Left: Spin-polarized HOMO−LUMO gap for the case CNT (11,0) as a function of length. The vacuum results are shown with black circles, and solvated results are shown in blue squares and red triangles. The bars indicate the standard deviation for each spin state. Inset: HOMO−LUMO gap as a function of time for the case CNT (11,0,7). The arrows on the right axis indicate the theoretically computed (open circle) and the experimentally measured (open diamond) band gap corresponding to a tube with infinite length. Right: Scheme of the absorption spectra proposed to be observed in vacuum labeled (a)(black lines), solvated labeled (b and c) (blue and red), and the convolution of the solvated spectra (green).

applications.[16] In addition, the energy difference between the antiferromagnetic state and a ferromagnetic state ($E_{FM} - E_{AFM}$) decreases with the length of the tube, changing from $\sim 20 k_B T$ for ~1.0 nm to $\sim 1 k_B T$ for length greater than ~3.0 nm (T = 298 K).[12] Another important aspect is that CNTs have remarkable optical absorption and fluorescence transitions, which have been shown to depend on the nanotube chirality, diameter, and length.[17] However, to experimentally observe these optical transitions from an individual nanotube, it is necessary to avoid the nanotube aggregation. This can be achieved by, for example, wrapping the tube with DNA[18−20] or surrounding the tube with a micelle of sodium dodecyl sulfate.[21]

Understanding the details on how the environment affects the electronic structure, e.g., changing the optical gap and the magnetic ordering in the CNT, will help the progress to use them in technological applications. Thus, the findings described before have motivated us to examine how the fluctuations in the environment, produced by the ubiquitous water molecules, influence the electronic properties of open-ended, finite-sized, single-walled zigzag CNTs with hydrogen atoms to passivate the edges (FS-CNT-H) using first-principle and classical molecular dynamics.

The key result of our work is the prediction that the degenerated HOMO−LUMO gap in FS-CNT-H occurring in vacuum is broken as soon as the tube is solvated with water molecules. Besides, the fluctuation during the molecular dynamics of the water molecules induces a fluctuation in the HOMO−LUMO gap. We examine in detail the electric field produced by both the confined water inside and the unconfined water outside of the CNT and how that field contributes to its electronic gap. In particular, we discuss the possibility to observe a change of the ground state of the solvated CNT from the semiconductor to metallic or half-metallic state.

COMPUTATIONAL DETAILS

We study open-ended finite-length zigzag CNTs terminated with hydrogen atoms, denoted as CNT (11,0,L), with L = 4, 7, and 10 zigzag rings along its axial axis with a corresponding length of 0.93, 1.56, and 2.20 nm, respectively, and with a diameter of 0.87 nm.

We first optimize the CNT in vacuum using first principles, and then we solvate the CNT with a box of water molecules and perform classical molecular dynamics. Finally, for some snapshots randomly selected from the molecular dynamics, we compute with QM/MM methods the electronic and magnetic properties of the solvated CNT. In this methodology, the CNT is treated in the QM part, with the first-principle screened exchange hybrid density functional of Heyd, Scuseria, and Ernzerhof (HSE),[22]and the water molecules in the MM part. In the Supporting Information, there is a complete description of the computational methodology, the results of the classical molecular dynamics of the solvated CNT, and the response of the CNT to the application of a uniform electric field. Overall, we find results similar to those previously reported by other authors (see ref 23 for a recent review), with respect to: (i) The filling of the CNT with water occurs as soon as the nanotube is embedded in a water reservoir. (ii) The transportation of confined water inside the CNT shows pulses (see Table S1 in the Supporting Information), whose direction flips from one open end to the other (see Figure S2 in the Supporting Information). Few flipping events were observed during the time of the molecular dynamics simulation where the confined water inside reverses the flow direction. (iii) The structure of confined water inside the nanotube is defined by hydrogen bond interaction among them, and the number of confined water molecules inside the nanotube is proportional to the number of rings (length) of the nanotube. (iv) Density profile for both bulk unconfined water outside the nanotube shows a depletion zone, followed by the first maximum, and then reaches bulk density. Also, (v) the time dependence of the dipole moment produced by confined water inside the nanotube is nearly along the axis of the nanotube and flips directions following the direction of flow. (vi) The dipole moment of all the unconfined water outside the nanotube shows a random behavior during the simulation. See the Supporting Information for more information. Thus, we assume hereafter that the water−CNT interaction is well described, and we can now focus on the computation of the changes in the electronic and magnetic properties induced by water molecules.

RESULTS AND DISCUSSION

Because the electronic properties of open-ended finite-sized CNTs depend, among others, on the length of the tube,[14] we analyze here how the HOMO−LUMO gap for each spin state

dx.doi.org/10.1021/jp308174k | J. Phys. Chem. C 2013, 117, 633−638

depends on it. First, we report results for CNT (11,0) in vacuum. We show in Figure 1 the HOMO−LUMO gap for the CNT (11,0) computed for different lengths (open circle). Our open-ended finite-sized CNT (11,0,L) is a semiconductor, and the α and β gaps are degenerated with a clear inverse dependence with the tube length, in agreement with the results published in ref 12 for short segments (L < 3.0 nm) of the CNT in vacuum, such as (7,0), (8,0), (9,0), and (10,0). Our results do not give us enough information to extrapolate to infinite length. We indicate with arrows and symbols the experimental band gap (1.19 eV)[24] reported for lengths of the CNT (11,0) beyond a few hundred of nanometers and also the theoretical value for an infinite CNT (1.05 eV) computed with the same functional used here.[25] As can be seen, for lengths beyond a few nanometers, the gap indeed reaches the value corresponding to infinite length. Now we inspect the solvent effect on the gap for the same tube length. To consider the effect of solvating the CNT on the HOMO−LUMO gap, we use QM/MM methods (see Supporting Information) to compute the electronic properties for a series of snapshots taken from the molecular dynamics simulations. We find that upon solvation the gap degeneracy is broken, and both spin states can be resolved for all the lengths studied. Figure 1 shows the mean value (triangles and squares) and its standard deviation σ_α and σ_β (bars) for the HOMO−LUMO gap of each spin state for the solvated CNT. Bars are between 50 and 120 meV with an average of ∼80 meV. We can inspect in detail the time dependency of the spin-polarized HOMO−LUMO gap computed with the QM/MM methodology. That is shown in the inset of Figure 1 for the particular case CNT (11,0,7). As seen, each spin state fluctuates around its corresponding mean value. The gap for each spin state can be better resolved for the CNT with the longest length studied here CNT (11,0,10). These theoretical results might be useful to understand an experimental optical spectrum of carbon nanotubes with length of the order of a few nanometers in vacuum and upon solvation. For illustrative purposes, we show in Scheme 1, at the left, the degenerated HOMO and LUMO energy levels for α and β spin corresponding to the vacuum situation. Thus, a single absorption spectrum would be observed (it is shown without broadening). At the right, the time fluctuation of the solvated molecules induces a fluctuating splitting of the HOMO and LUMO energy levels, and two broad absorptions (80 meV of broadening) would be observed.

Scheme 1. HOMO and LUMO Energy Levels for the Vacuum (Left) and Solvated (Right) CNT and the Corresponding Predicted Spectrum[a]

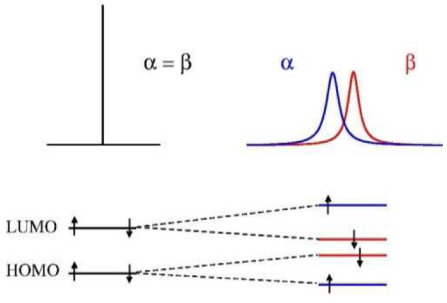

[a]The broadening is a consequence of the fluctuations in the energy levels.

To better visualize these results, we displayed at the right panel of Figure 1 the optical spectrum of a hypothetical sample containing three CNTs with the considered lengths. In vacuum (a), it is likely to expect a single electronic absorption peak for each CNT (black line) because α and β gaps are degenerated (no broadening was included). For the solvated CNTs (b), it is likely to expect for each CNT two peaks, one for each spin state (shown in colors). In green the convolution of the solvated spectra is shown. We used a Gaussian broadening with width of 80 meV to represent the dispersion of absorptions as predicted by the QM/MM methods. Presumably, as soon as the length increases, there will be more transitions around the theoretical value 1.05 eV, and as a consequence, a very intense signal will overlap the signal coming from finite-sized CNTs. This is consistent with the experimental finding that longer single-walled CNTs display stronger optical features.[14]

Induced Dipole Moment and the HOMO−LUMO Gap. We turn our attention now to the induced dipole moment on the CNT by the fluctuating water molecules because of its correlation with the electronic gap. Actually, in vacuum and in the absence of an external electric field, there is no net dipole moment in the studied CNTs, but it does appear upon solvation. In vacuum, a finite-sized CNT presents a non-homogeneous charge distribution where a similar amount of charge has accumulated in the two rings close to the edges and left the center almost uncharged. Thus, due to the symmetry of the charge distribution with respect to the center on the nanotube, the resulting net dipole moment is zero. Upon solvation, the charges on the nanotube move from one edge to the other one, breaking the symmetry in the charge distribution and resulting in a net induced dipole moment on the nanotube by the solvent, which we named μ^{ind}_{all}. In Scheme 2 we displayed with arrows the dipole moment of the confined water inside $\mu^{water}_{confined}$ and unconfined water outside $\mu^{water}_{unconfined}$ of the CNT and the corresponding response induced on the nanotube, $\mu^{ind}_{confined}$ and $\mu^{ind}_{unconfined}$, respectively. These are well-known results and can be compared with previous reports (see ref 26). Besides,

Scheme 2. Rectangle Representing a CNT and Arrows Indicating the Dipole Moment of the Confined Water Inside and Unconfined Water Outside the Nanotube and Also the Corresponding Induced Dipole Moment on a Solvated Nanotube[a]

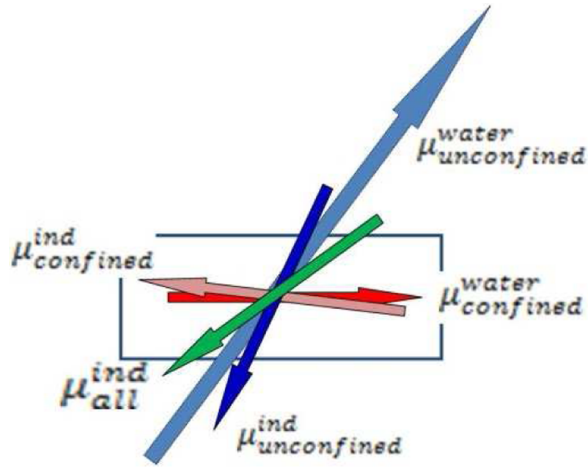

[a]The magnitude of the arrows is out of scale. The water molecules are omitted for clarity.

dx.doi.org/10.1021/jp308174k | J. Phys. Chem. C 2013, 117, 633−638

the fluctuations of the water molecules during the molecular dynamics cause the induced dipole moment on the nanotube to fluctuate as well.

We computed the total induced dipole moment on the CNT, μ_{all}^{ind}, as the sum of two contributions: one due to confined water inside the CNT, $\mu_{confined}^{ind}$, and the other from unconfined water outside the CNT, $\mu_{unconfined}^{ind}$.

The confined water molecules inside the CNT have a net dipole moment, $\mu_{confined}^{water}$, proportional to their number (see Table S1 in the Supporting Information). Here we discuss, as an example, the case for the CNT (11,0,7). We observe during the MD simulation between 4 and 8 confined water molecules inside the CNT, where 70% of the time we found 6 water molecules and 25% we found 7 water molecules. Thus, in average, $\mu_{confined}^{water}$ is 15.1 ± 1.3 D almost along the z-axis. These water molecules induce on the CNT $\mu_{confined}^{ind}$ = 7.9 ± 0.9 D, mainly pointing along the z-axis of the tube but in the opposite direction to $\mu_{confined}^{water}$. These dipole moments are shown in red and pink in Scheme 2. Meanwhile, the unconfined water outside (around 1030 water molecules) has a dipole moment $\mu_{unconfined}^{water}$ =189 ± 78 D (see Figure S2 in the Supporting Information) with a magnitude several times bigger than the confined water inside the CNT and with a random direction (blue arrow in Scheme 2). However, in spite of the different magnitude between $\mu_{confined}^{water}$ and $\mu_{unconfined}^{water}$, we found that $\mu_{unconfined}^{ind}$ is 9.6 ± 5 D. Therefore, the total induced dipole moment on the CNT of this particular size, μ_{all}^{ind}, can take values between 0 D, when $\mu_{confined}^{ind}$ is pointing in the opposite direction of $\mu_{unconfined}^{ind}$, and 24 D when $\mu_{confined}^{ind}$ is pointing in the same direction of $\mu_{unconfined}^{ind}$ (light blue arrow in Scheme 2). It is interesting to note that $\mu_{confined}^{ind}$ is nonzero most of the time, except when the CNT is empty which occurs within short intervals of time, and as a consequence $\mu_{confined}^{ind}$ defines a nearly constant background polarization.

We illustrate in Figure 2, with the same color used in Scheme 2, two different situations during the MD simulation for the

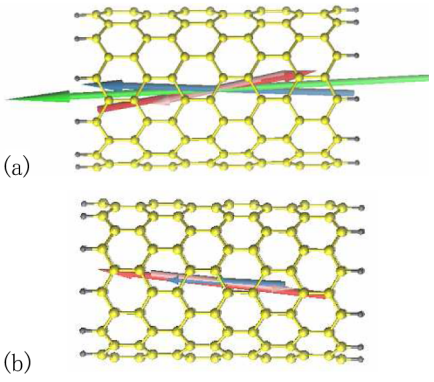

Figure 2. Dipole moment of the unconfined (blue), confined (red), and induced on the nanotube (green). The dipole moment of the unconfined water outside is omitted because it is 20 times bigger than the other moments. (a) Maximum induced dipole moment (24 D) and (b) minimum induced dipole moment (≈1 D). The water molecules were omitted for clarity.

CNT discussed above which correspond to: (a) a case with the maximum dipole moment induced on the CNT μ_{all}^{ind} ≈ 24 D, $\mu_{confined}^{ind}$ ≈ 8 D, $\mu_{unconfined}^{ind}$ ≈ 16 D, where the confined and unconfined dipoles have the same direction, and (b) a case with the minimum dipole moment induced on the CNT μ_{all}^{ind} ≈ 0.7 D, $\mu_{confined}^{ind}$ ≈ 8 D, $\mu_{unconfined}^{ind}$ ≈ 9 D, where the confined dipole has opposite direction to the unconfined one (see Figure S2 of the Supporting Information). In addition, Figure 2 displays the induced dipole moment produced by the confined water inside the nanotube $\mu_{confined}^{ind}$ and the induced dipole moment of the unconfined water outside of the nanotube $\mu_{unconfined}^{ind}$.

In Figure 3, we display the HOMO−LUMO gap as a function of the axial component (z) of the dipole moment

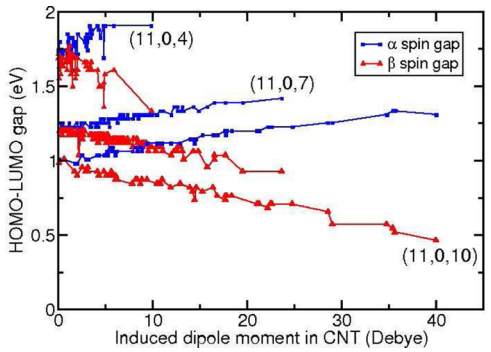

Figure 3. Spin-polarized HOMO−LUMO gap of a CNT (11,0) with 4, 7, and 10 zigzag rings as a function of the induced dipole moment projected along the axial axis. The maximum induced dipole moment for each length is 10, 24, and 40 D.

induced on the CNT by all the water molecules present in the simulation box computed with QM/MM methods for the different lengths considered for the three sizes of CNTs. As expected, the longest CNT (11,0,10) responds to the electric field produced by the water molecules with larger polarization.[27,28]

As seen in Figure 3, the HOMO−LUMO gap for both spin states has a nearly linear dependence with the induced dipole moment, presenting a response similar to the application of a uniform external electric field along the axial axis.[12] That is, one spin state increases, whereas the other spin state decreases (see Figure S5 in the Supporting Information). Meanwhile, the HOMO−LUMO gap for both spin states remains degenerated with the transverse component of the induced dipole moment (data not shown). To rationalize the relation between the induced dipole moment on the CNT and the electric field produced by the water molecules, we compute (see Figure S5 in the Supporting Information) the induced dipole moment as a function of a uniform electric field applied along the axial and transverse axis for each CNT studied here. We observe a linear dependence between the induced dipole and the external electric field for both axial and transverse directions for values of the electric field lower than 2 V/nm .

On the basis of that linear relation and using the maximum induced dipole moment shown in Figure 3 (also Figures S4 and S5 in the Supporting Information), we found that the maximum induced dipole moment along the axial axis corresponds to the application of a uniform electric field of ∼1.7 ± 0.2 V/nm. We then conclude that the maximum electric field produced by the water molecules should be similar to that value. In addition, the electric field produced by the confined water inside the nanotube is equivalent to an external uniform electric field with a mean value of 0.56 V/nm with a fluctuation of ±0.05 V/nm. Meanwhile, the unconfined water outside the nanotube produces a random electric field, equivalent to an external uniform electric field with a mean value of 0.7 V/nm with a fluctuation of ±0.4 V/nm. The maximum electric field observed is ∼3 times smaller than the one needed to turn the

dx.doi.org/10.1021/jp308174k | J. Phys. Chem. C 2013, 117, 633−638

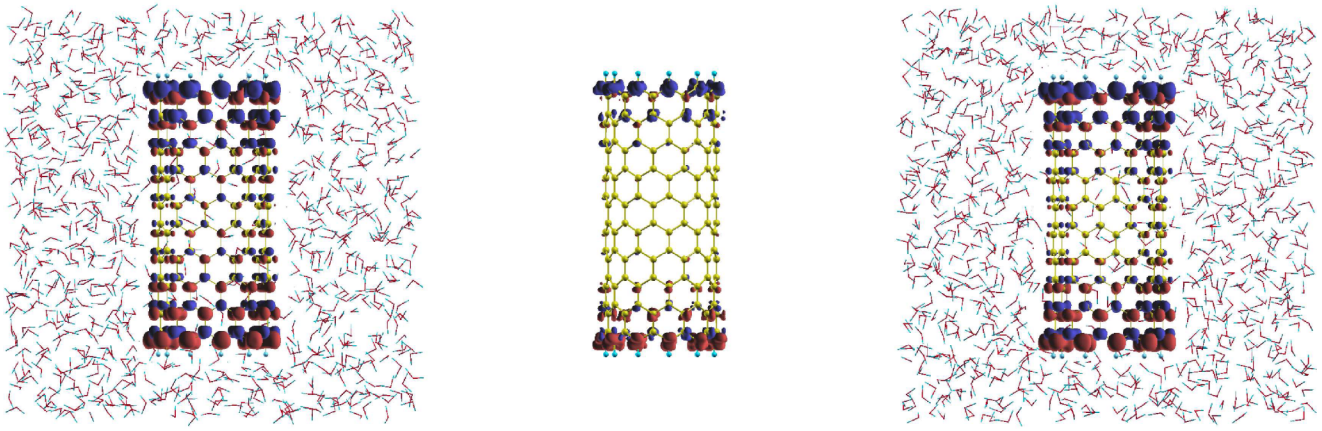

Figure 4. Spin density maps of the (11,0,10) for two different snapshots corresponding to the smaller (left) and bigger (right) induced dipole moment. The spin density map at the center is the difference of the two previous densities, and the water molecules are not shown for clarity. The α spin density is in blue, and β spin density is in red.

CNT to half-metallic (see Figure S6 in the Supporting Information) and can be compared with the observed values at the active site of proteins which is around 1.1 V/nm and for a fragment of grapheme embedded in water which is 1.6 V/nm.[29,30]

Spin Polarization at the Edges. As mentioned before in vacuum, the ground state of the finite-sized CNT (11,0,L) studied here is antiferromagnetic with one edge having high population of spin density α and the opposite edge having high population of spin density β. This also occurs after solvating the CNT, but in addition, the spin density fluctuates responding to the fluctuations of the electric field of the surrounding molecules. To illustrate that, in Figure 4 we show the spin density (blue α and red β spin) of the CNT (11,0,10) for two different snapshots, when the induced dipole moment has a minimum (left panel) and a maximum value (right panel). To emphasize the change in the spin density, we show in the center panel the difference of those situations. As can be seen, there is an enhancement of the α and β spin density at the edges, while the spin density located at the center of the tube remains almost unchanged.[31] The change in the electronic spin polarization arises from the carbon 2π orbitals which are pointing perpendicular to the CNT surface and are polarized by the surrounding water molecules. In particular, for the case (11,0,7), $E_{FM} - E_{AFM}$ is 0.53 eV ($\sim 20\ k_BT$) with the $m_s = 4$, and for the case (11,0,10), $E_{FM} - E_{AFM}$ is 0.16 eV ($\sim 6k_BT$), with the $m_s = 4$ as the above lying ferromagnetic state in vacuum and solvated ($T = 298$ K). Figure S3 in the Supporting Information shows $E_{FM} - E_{AFM}$ as a function of length for different m_s.

SUMMARY AND CONCLUSIONS

We have studied the changes in the electronic properties of open-ended zigzag finite-sized hydrogen-terminated CNTs embedded in water molecules within density functional theory combined with molecular mechanics and classical molecular dynamics. Considering that in short CNTs the self-interaction energy has to be computed as precise as possible, we have used the screened hybrid functional HSE for our work. This has allowed us to compute the correct ground state magnetization and a reliable electronic band gap in vacuum, and the embedded CNT for a set of randomly selected snapshots was taken from the classical molecular dynamics simulations. Our results can be summarized as follows: (i) the degenerated HOMO−LUMO gap observed in vacuum is broken when the CNT is solvated with water molecules; (ii) it decreases when the CNT length increases; (iii) the α and β gaps fluctuate in response to the fluctuations of the water molecules during the molecular dynamics simulation but still can be resolved; (iv) in response to the fluctuating electric field produced by the solvent, a fluctuating induced dipole moment is observed; (v) the maximum electric field produced by the solvent is 1.7 ± 0.2 V/nm which results from the addition of the electric field produced by the confined water inside and unconfined water outside the CNT; and (vi) confined water molecules produce on the tube a nearly constant electric field and nearly along the z-axis of the nanotube, while the unconfined water produces an electric field with random magnitude and direction.

We did not observe a change due to the solvation in the ground state magnetic polarization for the tubes of different lengths studied here, but we speculate that for a length of 3 nm for which the $E_{FM} - E_{AFM}$ is of the order of $1k_BT$, a change in the magnetic polarization could be observed.

We hope that these findings may have some relevance when open-ended finite-sized CNTs are employed in nanotechnological devices where solvent molecules are present and changes in the electronic properties are relevant.

ASSOCIATED CONTENT

Supporting Information

Complete description of the computational methods and classical molecular dynamics. This material is available free of charge via the Internet at http://pubs.acs.org.

AUTHOR INFORMATION

Corresponding Author

*E-mail: dalosto@intec.unl.edu.ar.

Notes

The authors declare no competing financial interest.

ACKNOWLEDGMENTS

This work was supported by grants No. PICT-2007-317, PICT-PRH-195, and PICT-PRH-99 from ANPCyT Argentina. C.M.R. acknowledges a fellowship from ANPCyT- PICT-2007-317. We thank Silvia Tinte (INTEC) for the proofreading of the manuscript.

REFERENCES

(1) Serp, P.; Castillejos, E. *ChemCatChem* **2010**, *2*, 41−47.
(2) Mitchell, D. T.; Lee, S. B.; Trofin, L.; Li, N.; Nevanen, T. K.; Söderlund, H. S.; Martin, C. R. *J. Am. Chem. Soc.* **2002**, *124*, 11864−11865.
(3) Holt, J. K.; Park, H. G.; Wang, Y.; Stadermann, M.; Artyukhin, A. B.; Grigoropoulos, C. P.; Noy, A.; Bakajin, O. *Science* **2006**, *312*, 1034−1037. Kalra, A.; Garde, S.; Hummer, G. *Proc. Natl. Acad. Sci. U.S.A* **2003**, *100*, 10175−10180. Kreuer, K.-D.; Paddison, S. J.; Spohr, E.; Schuster, M. *Chem. Rev.* **2004**, *104*, 4637−4678. Corry, B. *J. Phys. Chem. B* **2008**, *112*, 1427−1434.
(4) Li, J.; Gong, X.; Lu, H.; Li, D.; Fang, H.; Zhou, R. *Proc. Natl. Acad. Sci. U.S.A.* **2007**, *104*, 3687−3692. Liu, L.; Qiao, Y.; Chen, X. *Appl. Phys. Lett.* **2008**, *92*, 101927. Zuo, G.; Shen, R.; Ma, S.; Guo, W. *ACS Nano* **2010**, *4*, 205−210.
(5) Kyakuno, H.; Matsuda, K.; Yahiro, H.; Inami, Y.; Fukuoka, T.; Miyata, Y.; Yanagi, K.; Maniwa, Y.; Kataura, H.; Saito, T.; Yumura, M.; Iijima, S. *J. Chem. Phys.* **2011**, *134*, 244501.
(6) Thomas, J. A.; McGaughey, A. J. H. *J. Chem. Phys.* **2008**, *128*, 084715.
(7) Wang, H. J.; Xi, X. K.; Kleinhammes, A.; Wu, Y. *Science* **2008**, *322*, 80−83.
(8) Joseph, S.; Aluru, N. R. *Nano Lett.* **2008**, *8*, 452−458.
(9) Holt, J. K.; Park, H. G.; Wang, Y.; Stadermann, M.; Artyukhin, A. B.; Grigoropoulos, C. P.; Noy., A.; Bakajin, O. *Science* **2006**, *312*, 1034−1037.
(10) Rasaiah, J. C.; Garde, S.; Hummer, G. *Annu. Rev. Phys. Chem.* **2008**, *59*, 713−740.
(11) Ezawa, M. *Phys. Rev. B* **2007**, *76*, 245415.
(12) Hod, O.; Peralta, J. E.; Scuseria, G. E. *Phys. Rev. B* **2007**, *76*, 233401.
(13) Ezawa, M. *Phys. E* **2008**, *40*, 1421−1423.
(14) Hod, O.; Scuseria, G. E. *ACS Nano* **2008**, *2*, 2243−2249.
(15) Fernandez-Rossier, J.; Palacios, J. *J. Phys. Rev. Lett.* **2007**, *99*, 177204.
(16) Žutić, I.; Fabian, J.; Das Sarma, S. *Rev. Mod. Phys.* **2004**, *76*, 323−410.
(17) Fagan, J. A.; Simpson, J. R.; Bauer, B. J.; Lacerda, S. H. D. P.; Becker, M. L.; Chun, J.; Migler, K. B.; Walker, A. R. H.; Hobbie, E. K. *J. Am. Chem. Soc.* **2007**, *129*, 10607−10612.
(18) Huang, X.; Mclean, R. S.; Zheng, M. *Anal. Chem.* **2005**, *77*, 6225−6228.
(19) Cathcart, H.; Nicolosi, V.; Hughes, J. M.; Blau, W. J.; Kelly, J. M.; Quinn, S. J.; Coleman, J. N. *J. Am. Chem. Soc.* **2008**, *130*, 12734−12744.
(20) Zheng, M.; Jagota, A.; Semke, E. D.; Diner, B. A.; McLean, R. S.; Lustig, S. R.; Richardson, R. E.; Tassi, N. G. *Nat. Mater.* **2003**, *2*, 338−342.
(21) O'Connell, M. J.; Bachilo, S. H.; Huffman, C. B.; Moore, V. C.; Strano, M. S.; Haroz, E. H.; Rialon, K. L.; Boul, P. J.; Noon, W. H.; Kittrell, C.; Ma, J.; Hauge, R. H.; Weisman, R. B.; Smalley, R. E. *Science* **2002**, *297*, 593−596.
(22) Heyd, J.; Scuseria, G. E.; Ernzerhof, M. *J. Chem. Phys.* **2003**, *118*, 8207−8215.
(23) Kofinger, J.; Hummer, G.; Dellago, C. *Phys. Chem. Chem. Phys.* **2011**, *13*, 15403−15417. Berezhkovskii, A.; Hummer, G. *Phys. Rev. Lett.* **2002**, *89*, 064503.
(24) Ma, Y,-Z.; Valkunas, L.; Bachilo, S. M.; Fleming, G. R. *J. Phys. Chem. B* **2005**, *109*, 15671.
(25) Brothers, E. N.; Scuseria, G. E.; Kudin, K. N. *J. Phys. Chem. B* **2006**, *110*, 12860.
(26) Lu, D.; Li, Y.; Rotkin, S. V.; Ravaioli, U.; Schulten, K. *Nano Lett.* **2004**, *4*, 2383−2387.
(27) Benedict, L. X.; Louie, S. G.; Cohen, M. L. *Phys. Rev. B* **1995**, *52*, 8541−8549.
(28) It is worth mentioning that the CNTs are fixed during the simulations, thus the induced polarization is entirely electronic. However, allowing the relaxation of the CNT, in order to take into account the structural contribution to the induced dipole moment, only changes 4%.
(29) Fafarman, A. T.; Sigala, P. A.; Schwans, J. P.; Fenn, T. D.; Herschlag, D.; Boxer, S. G. *Proc. Natl. Acad. Aci. U.S.A.* **2012**, *109*, E299−E308.
(30) Dalosto, S.; Tinte, S. *J. Phys. Chem. C* **2011**, *115*, 4381−4386.
(31) This enhancement could be quantitatively different if the LSDA functional is used because of its poor description of the self-interaction which is partially solved with the hybrid functional HSE used in our work.